

# Correct D<sub>2</sub>O Cold Fusion Reactor with Strong Alkaline Electrolyte

## (Heat Generating Metal Needs to be Anode)

Noriyuki Kodama  
Independent Researcher

**Abstract:-** Fleischmann and Pons discovered that cold fusion occurs when metal electrodes are treated under heavy water under electrolysis conditions, but the reproducibility was initially very low. The Cold Fusion occurs by the compression of D<sub>2</sub> atoms at the expandable T site on the nano-roughness of the FCC metal. Compressed D<sub>2</sub> molecule is transition to femto-D<sub>2</sub> molecules which electron orbit is deep orbit deeper than  $n=1$  at a few femto meter from the nucleus. Because the density of electron between the nucleus is so high that it can shield the coulomb repulsive force between the nuclei. The expandable T site is on the nano-roughness of the FCC metal surface, which vertex atom of T site can have no bond to the atom of the adjacent lattice. Therefore, that vertex atom can move, and it is expandable. Center of the expandable T site is negatively charged due to the electronegativity of metal atoms. Thus, under positive voltage of metal, D becomes D<sup>+</sup> due to its smaller size and positive potential, and D<sup>+</sup> is attracted by the negative charge of the expandable T site and occupy the expandable T site and turn into D<sup>-</sup> which expand the T site due to the larger size of D<sup>-</sup>, and again another D<sup>+</sup> is attracted by D<sup>-</sup> and join to be D<sub>2</sub> at the expanded T site.

Although FCC metal need to be positive voltage based on the mechanism of Cold fusion, Fleischmann and Pons experimental set up is that FCC metal plate is negative voltage and all of the experiments have used the original incorrect setting of voltage.

Based on the above mechanism of Cold Fusion the behavior of deuterium in a D<sub>2</sub>O-based strong alkaline electrolyte show that in case of PH=11 [D<sup>+</sup>] = 10<sup>-11</sup> mol/l, [OD<sup>-</sup>] = 10<sup>-3</sup> mol/l, the [OD<sup>-</sup>] concentration is overwhelmingly high, and electrolysis proceeds easily.

Under the incorrect voltage conditions, the heat generation of the vapor is 4 to 190mW, however, the correct voltage condition can have the heat can be 100kW for the very small experimental setting.

Therefore, we can develop Cold Fusion Reactor with 1MWh at least on the desk top size, and it can replace plasma nuclear fusion reactor and nuclear power.

**Keywords:-** LENR, ColdFusion, LiOD, D<sub>2</sub>O.

## I. INTRODUCTION

I have reported the mechanism of Cold fusion in ref [1], which show that heat generating metal need to be positive potential, however, most reactors have not followed the mechanism of Cold Fusion, Since the Fleischmann and Pons reported the cold fusion, heating metal have been cathode (negative voltage).

## II. MECHANISM OF COLD FUSION

### A. Electron Deep Orbit (EDO) Theory

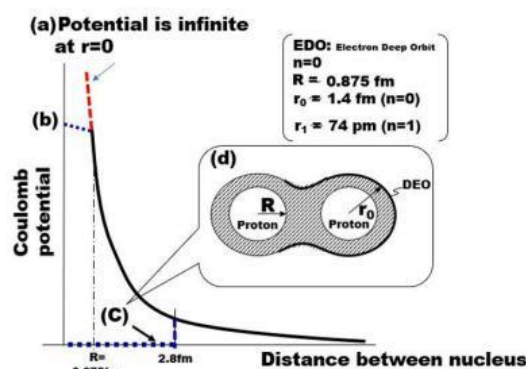
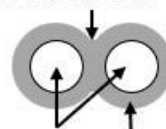


Fig.1. femto-H<sub>2</sub> with Electron Deep Orbit (EDO), in ref[2]-[14]

### (1) femto-D<sub>2</sub>



### (2) femto-H<sub>2</sub> Covalent Bond



### Electron Deep Orbit

Fig.2 Structure of femto-H<sub>2</sub> and femto-D<sub>2</sub>

Cold fusion occurs by the femto- $D_2$  molecule with electron orbit at a few femto meters from the nucleus(fig.1(d)), reported in ref [1]. Because the covalent electron density of femto- $D_2$  is so dense that it can shield the coulomb repulsive force between nuclei (Fig.2(1)).

### B. Expandable T Site

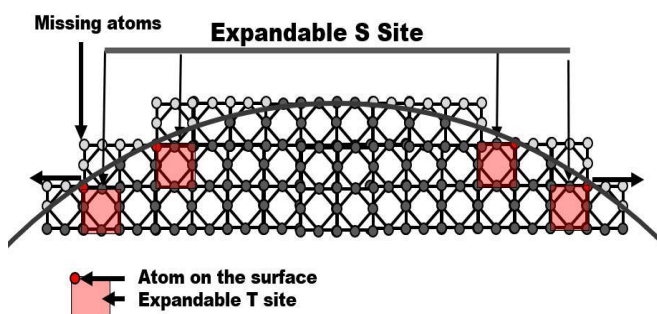


Fig.3 Expandable T site on the surface of metal

Cold fusion occurs on the nano-roughness of the FCC metal surface. Such surface has the expandable T site shown in Fig.3.

Because the Lattice on the surface can have the vertex metal atoms without any bond to the adjacent metal atoms in the adjacent lattice, T site with such vertex atom can be expanded by moving such vertex atom.

### C. Femto- $D_2$ generation at expandable T site

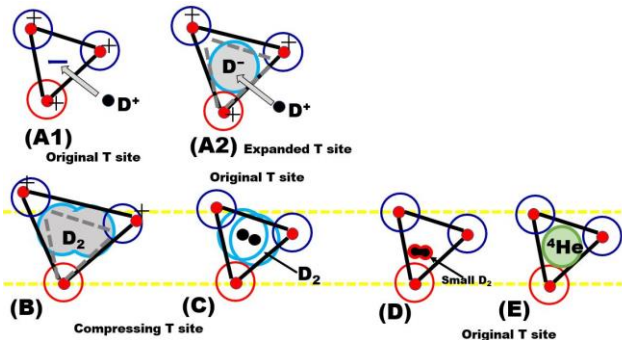


Fig.4 Mechanism of  $D^-$  occupation and cold fusion by bond compression at T site as is shown in Fig.3.

As is shown in Fig.4(A1), at the center of expandable T site is negatively charged because metal atom of T site tend to emit electron due to its electronegativity. In case of positive metal potential, D can be  $D^+$  in the metal and on the metal in case that the surface potential of metal is also positive. Therefore,  $D^+$  can be attracted by the negative charge at the expandable T site, and it becomes  $D^-$ , and attracted another  $D^+$  around  $D^-$  and they join to be  $D_2$  molecules at the expanded T site, as is shown in Fig.4 (B).

$D_2$  covalent bond is compressed by the surrounding metal atoms at the expanded T site, shown in Fig.4(B)-(C), and compression of covalent bond of  $D_2$  cause the electron transition from  $n=1$  to deep electron orbit, shown in Fig.4(D).

Because deep electron orbit can shield the coulomb repulsive force between nuclei, femto- $D_2$  can cause Cold Fusion, shown in Fig.4(E).

It is important to understand that Cold Fusion need the positive potential.

### D. Selecting a Template (Heading 2)

## III. INCORRECT COLD FUSION REACTOR

### A. Correct Electrolysis condition

Hydrogen generation by electrolysis of Water lately has been developed extensively, and standard condition.

Under these conditions, the concentration of  $[OH^-]$  in the aqueous solution is extremely high, and it adsorbs to the surface of the positive electrode, where it separates into  $H^+$  and  $O^-$ .

Under this electrolysis condition, the electrolysis rate is very fast because of the high conductivity of  $H_2O$ .

### B. Incorrect Condition Of $D_2O$ In Strong Alkaline Electrolyte

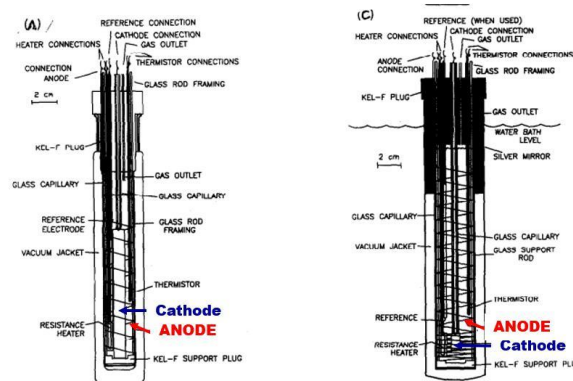


Fig.5 Experimental setup by Fleischmann and Pons[15]

In FIG. 5, the wire anode is arranged so that the cathode of Pd metal plate is surrounded by wire anode. Since the heating metal needs to be positive voltage, this experimental set-up is incorrect based on Cold Fusion mechanism.

### C. Summary of latest $D_2O$ Cold Fusion Reactor

It appears that incorrect potential has not yet been corrected. There are similar errors in other literature.[1]

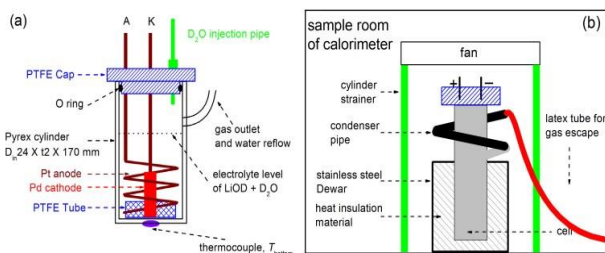


Fig.6 Schematics of Pd- $D_2O$  reflux open-electrolytic cell (a) and the cell with calorimetric attachment (b). in ref[16]

As is shown in Fig.6(a), Pd cathode and Pt anode are incorrect up to 2023.

Table 2. Summary of excess heat in the Pd(Pt)-D<sub>2</sub>O+LiOD open-electrolytic cell from 2018 to 2019.

Exp. #	$I \times t$ A × h	Integrated values			Steady values							
		$Q_{in}$ kJ	$Q_{ex}$ kJ	$P_{ex}$ mW	$I$ mA	$P_{in}$ W	$P_{ex}$ mW	$T_{bottom}$ °C	$T_{top}$ °C	$P_{vapor}$ mW		
180911Pt	0.17×48	148.89(33)	-0.49(71)	-2(3)	171	0.381(1)	6(2)	48	NA	NA		
	0.34×24				340	0.942(2)	-19(3)	73	NA	NA		
181005Pt	0.17×60	114.68(30)	0.35(60)	2(3)	171	0.521(1)	12(3)	51	41	4		
					171	0.539(3)	-1(3)	53	42	5		
181017Pt	0.17×60	125.69(35)	0.64(63)	3(3)	171	0.578(2)	2(2)	48	39	4		
					171	0.573(1)	7(2)	50	39	4		
190414Pt	0.17×60	134.83(14)	-0.27(80)	-1(4)	170	0.614(2)	-7(3)	52	40	4		
					170	0.638(2)	-4(3)	55	40	4		
190502Pt	0.17×60	139.021(14)	-0.23(80)	-1(4)	171	0.638(1)	0(3)	51	41	4		
					171	0.631(1)	5(3)	51	41	4		
190507Pt	0.34×54	322.23(15)	-0.74(76)	-4(4)	341	1.566(2)	3(3)	76	63	31		
190513Pt	0.51×19	239.50(7)	6.32(32)	92(5)	511	3.075(16)	178(20)	93	87	252		
190816Pt	0.51×36	191.98(10)	-0.73(56)	-6(4)	511	1.423(4)	5(4)	72	52	25		
					511	1.500(3)	5(3)	74	53	26		
190904Pd3	0.15×24	188.77(10)	-6.71(52)	-78(6)	148	2.029(115)	-65(17)	82	67	17		
					148	2.216(111)	-97(111)	87	69	20		
190909Pd3	0.34×22	120.30(5)	-0.27(53)	-3(7)	340	1.207(38)	9(10)	69	50	15		
190920Pd3	0.31×60	483.64(17)	-4.58(268)	-21(12)	228	1.522(97)	-24(19)	78	52	11		
					228	2.006(59)	36(86)	85	63	21		
191005Pd3	0.51×24	191.98(8)	1.64(134)	19(16)	511	2.212(13)	32(27)	78	65	52		
					550	3.060(15)	132(50)	87	76	118		
191007Pd3	0.55×48	543.64(15)	14.79(220)	86(13)	550	3.381(44)	88(44)	87	77	125		
					541	4.081(15)	182(33)	90	83	190		
191010Pd3	0.47×48	619.40(17)	20.63(225)	119(13)	360	3.317(24)	46(19)	84	71	55		

\* Meanings of symbols:  $I$ , electrolysis current;  $t$ , electrolysis time;  $Q_{in}$ , input energy;  $Q_{ex}$ , excess heat;  $P_{ex}$ , excess power;  $T_{bottom}$ , cell-bottom temperature;  $T_{top}$ , cell-top temperature;  $P_{vapor}$ , evaporation power of heavy water at  $T_{top}$  [3,2,5-8].

Fig.7 Summary of excess heat in the Pd (Pt)-D<sub>2</sub>O+LiOD open-electrolytic cell from 2018 to 2019.in ref [16].

The above reference [16] is a paper presented at ICFF-23, a conference held in 2021, but the electrode potential conditions in the LiOD + D<sub>2</sub>O electrolyte are Pd as the cathode and Pt as the anode, are still incorrect.

This is because none researchers have not understood the correct mechanism of Cold fusion presented by my previous papers. [1]

#### D. Comparison between correct potential and incorrect potential for Cold Fusion

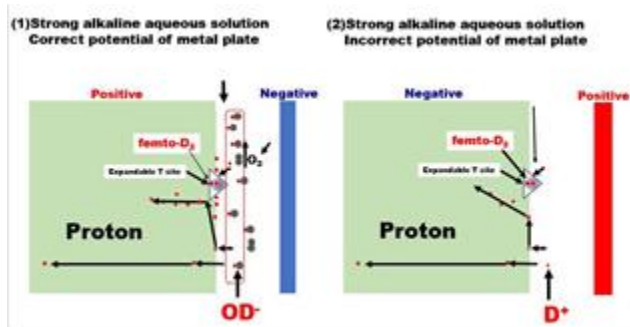


Fig.8 metal potential and D+ loading

$[D^+] \times [OD^-] = 1.0 \times 10^{-14}$  (mol/L)<sup>2</sup>(ionic product of heavy water)

Therefore, under strong alkaline conditions,  $[H^+]$  becomes very small, and basically it takes a very long time for palladium to fully absorb deuterium.

If PH = 11,  $[OD^-] \times [D^+] = 10^{-14}$  mol/l, so  $[D^+] = 10^{-11}$  mol/l and  $[OD^-] = 10^{-3}$  mol/l. thus  $10^{-3}/10^{-11}=10^8$  times.

Under the summary of heat generation in Fig.7,  $P_{vapor}$  is 0 to 190 mW, which is extremely small.

Estimated  $P_{vapor}$  based on correct potential is as high as  $10^5$  W = 100 kW by estimation with ratio of  $10^8$ .

These experimental set-ups are very small and desk-top type reactor, thus proper design of D<sub>2</sub>O cold Fusion Reactor can produce can generate very large amount of heat.

#### IV. CONCEPTUALIZED COLD FUSION REACTOR WITH STRONG ALKALINE ELECTROLYTE

##### A. Grain-boundary segregation of D to improve the reaction rate

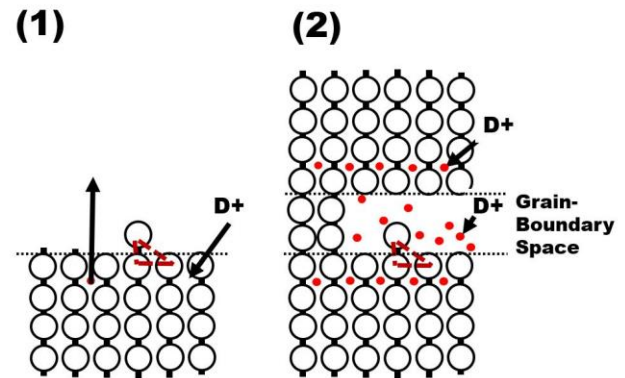


Fig.9 Mechanism to improve reaction rate to segregate D<sup>+</sup> at the grain boundary[17]

In order to improve the reaction rate, palladium polycrystalline thin film on the ceramics is proposed. Due to the segregation of D<sup>+</sup> at the grain boundary, it can enter the Expandable T site at grain boundary sidewall. Because conventional Cold Fusion use the metal surface, the reaction rate is very low due to the less D<sup>+</sup> around Expandable T site.

##### B. Efficient trigger of Cold Fusion

The issue of D<sub>2</sub>O-based cold fusion heat generators is that the metal is directly cooled by D<sub>2</sub>O, so the temperature of 700 degrees for triggering cold fusion cannot reach that value if a normal ceramic heater is used.

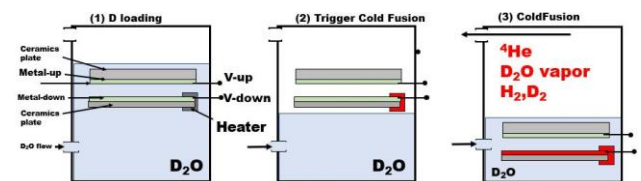


Fig.10 D<sub>2</sub>O cold Fusion Reactor to trigger Cold Fusion

- D loading
- Trigger Cold Fusion
- Cold Fusion

Thin films of polycrystalline palladium and platinum are formed on a ceramic substrate, and the palladium film is so thin to saturate the D<sup>+</sup> concentration inside the film to segregate D<sup>+</sup> to the grain boundary.



The potential of palladium is positive and potential of Pt is negative to load  $D^+$  and cold fusion simultaneously.

At the time of cold fusion trigger, the liquid level is set to be lower than the heat-generating metal so that metal temperature can be high without cooling the metal. Under these conditions, the temperature can be easily raised to about 700 degrees with a ceramic heater.

After the trigger of Cold Fusion, there is a risk that the temperature will rise further and the metal will melt, so the position of the metal substrate is lowered as in (3) to cool it instantly.

## V. SUMMARY

Current D2O Cold Fusion Reactor has incorrect metal potential setting. Heat generating metal need to be positive based on the Cold Fusion mechanism.

Rough estimation shows that heat generation will be = 100 kW for the desk top experimental setting. Therefore, it can have the low cost and safer with small volume power generation.

## REFERENCES

- [1]. Noriyuki Kodama, Novel Cold Fusion Reactor with Deuterium Supply from Backside and Metal Surface Potential Control, Volume6, Issue 6, June-2021 International Journal of Innovative Science and Research Technology Also available from <https://ijisrt.com/novel-cold-fusion-reactor-with-deuterium-supply-from-backside-and-metal-surface-potential-control>
- [2]. J. Va'vra, ON a possibility of existence of new atomic levels, which were neglected theoretically and not measured experimentally.
- [3]. A. Meulenberg, K. P. Sinha, Deep-electron Orbits in Cold Fusion, J. Condensed Matter Nucl. Sci. 13 (2014) 368–377,
- [4]. J. Va'vra, A simple argument that small hydrogen may exists, Phys. Lett. B, 794 (2019) 130-134. Also available from <https://arxiv.org/ftp/arxiv/papers/1906/1906.08243.pdf>
- [5]. J.L. Paillet, On highly relativistic deep electrons, J. Condens. Matter Nucl. Sci. 29 (2019) 472–492. Also available from <https://www.vixra.org/pdf/1902.0398v1.pdf>.
- [6]. J.-L. Paillet, A. Meulenberg, Basis for EDOs of the hydrogen atom, Proc. 19th International Conference on Condensed Matter Nuclear Science, Padua, Italy, 13-17 April 2015. Also available from <https://www.proceedings.com/30912.html>
- [7]. J. Maly and J. Va'vra, Electron transitions on deep Dirac levels I, Fusion Technol., 24 (1993) 307-318. Also available from <https://doi.org/10.13182/FST93-A30206>
- [8]. J. A. Maly, J. Vavra, Electron transitions on deep Dirac levels II, Fusion Technol. 27 (1995) 59-70. Also available from <https://doi.org/10.13182/FST95-A30350>
- [9]. J. Va'vra, On a possibility of existence of new atomic levels, which were neglected theoretically and not measured experimentally, presented at Siegen University, Germany, November 25, 1998.
- [10]. J. Va'vra, A new way to explain the 511 keV signal from the center of the Galaxy and some dark matter experiments, ArXiv: 1304.0833v12 [astro.ph-IM] Sept. 28, 2018. Available from
- [11]. <https://doi.org/10.48550/arXiv.1304.0833>
- [12]. J.-L. Paillet, A. Meulenberg, Highly relativistic deep electrons and the Dirac equation, J. Cond. Matter Nucl. Sci. 33 (2020) 278–295. Also available from [https://www.academia.edu/41956585/Highly\\_relativistic\\_deep\\_electrons\\_and\\_the\\_Dirac\\_equation](https://www.academia.edu/41956585/Highly_relativistic_deep_electrons_and_the_Dirac_equation).
- [13]. Z.L. Zhang, W.S. Zhang, Z.Q. Zhang, Further study on the solution of schrödinger equation of hydrogen-like atom, Proc. 9th International Conference on Cold Fusion, May 21-25, 2002, Beijing, China, pp. 435-438. Available from [https://lenr-canr.org/wordpress/?page\\_id=691](https://lenr-canr.org/wordpress/?page_id=691)
- [14]. A. Meulenberg, Deep-orbit-electron radiation absorption and emission, Available From <https://mospace.umsystem.edu/xmlui/bitstream/handle/10355/36501/DeepOrbitElectronRadiationAbstract.pdf?sequence=1&isAllowed=y>
- [15]. A. Meulenberg, J.L. Paillet, Implications of the EDOs for cold fusion and physics–deep-orbit-electron models in LENR: Present and Future, J. Condens. Matter Nucl. Sci. 24 (2017) 214–229
- [16]. S. Pons, M. Fleischmann, S. Pons, "Some comments on the paper Analysis of Experiments on Calorimetry of LiOD/D<sub>2</sub>O Electrochemical Cells, R.H., J. Electroanal. Chem., 332 (1992)
- [17]. [https://www.newenergytimes.com/v2/library/1992/1992\\_FleischmannM-SomeComments.pdf](https://www.newenergytimes.com/v2/library/1992/1992_FleischmannM-SomeComments.pdf)
- [18]. Hui Zhao, Wu-Shou Zhang,, Wu-Yun Xiao, Yang Sun1, Excess heat in a Pd(Pt)-D2O+LiOD reflux open-electrolytic cell, in ICCF-23 June 9th-11th, 2021,
- [19]. <https://lenr-canr.org/acrobat/ZhaoHexcessheat.pdf>
- [20]. Noriyuki Kodama, Conceptualized Cold fusion reactor with improved reaction rate by segregating deuterium at grain boundaries,
- [21]. Noriyuki Kodama, Conceptualized Cold fusion reactor with improved reaction rate by segregating deuterium at grain boundaries, Volume 8, Issue 5, May (2023) in International Journal of Innovative Science and Research Technology,
- [22]. <https://ijisrt.com/assets/upload/files/IJISRT23MAY667.pdf>